Direct Shear Bond Tests of Fabric-Reinforced Cementitious Matrix Materials

Francesca Giulia Carozzi[1]; Diana Arboleda, A.M.ASCE[2]; Carlo Poggi[3]; and Antonio Nanni, F.ASCE[4]

Abstract: Fabric-reinforced cementitious matrix (FRCM) composites consist of a dry fiber fabric embedded in an inorganic mortar that may be enriched with short fibers. These composites are particularly well-suited for the strengthening of historical buildings due to their high compatibility with the substrate, vapor permeability, and durability. One of the most critical factors influencing the effectiveness of a composite applied externally to masonry or concrete structures is debonding of the system from the substrate. In FRCM systems, the failure is often localized at the mortar–fabric interface. This paper presents a summary of experimental investigations of the bond properties of six different FRCM systems in various configurations of bond length and substrate material. Finally, some considerations and indications for inclusion of the test procedure in guidelines and acceptance criteria are presented. **DOI: 10.1061/(ASCE)CC.1943-5614.0000991.**

Author keywords: Bond testing; Fabric-reinforced cementitious matrix; Repair; Strengthening.

Introduction

External structural repair methods extend the life of the built stock while enhancing its safety. To realize such potential benefits, engineers rely on design guidelines established after extensive research studies on material behavior have been performed and simplified behavioral models have been developed and validated. The characterization of fabric-reinforced cementitious matrix (FRCM) systems has contributed significantly to their advancement as a proven technology for structural rehabilitation. FRCM composites consist of one or more layers of dry fiber fabric reinforcement embedded in an inorganic matrix made of a cementitious or lime-based mortar enriched with a low dosage of short fibers and additives. The fabric is considered to be bare because its fibers are not completely impregnated with resin, although fiber yarns can have an external coating for protection or to enhance bonding to the matrix. In any case, fibers internal to a yarn can transfer stresses among each other only by friction.

One of the most important aspects influencing the effectiveness of any external strengthening system is the adhesion between the system and the substrate, and between fabric and matrix at its interface when using FRCM. In this paper, a test method to complement the characterization of FRCM is presented along with a simplified analytical model calibrated to the experimental results of the test aimed at enhancing design guidelines and acceptance criteria. First, an overview of bond test methods and bond performance of FRCM systems is presented; then, an experimental evaluation of the adhesion characteristics of several FRCM systems is discussed, followed by an analysis. Finally, a proposal for the inclusion of this method in acceptance criteria for system certification is given.

[1]Research Assistant, Dept. of Architecture, Built Environment, and Construction Engineering, Politecnico di Milano, Piazza Leonardo da Vinci 32, Milano 20133, Italy (corresponding author). Email: francescagiulia.carozzi@polimi.it

[2]Lecturer, Dept. of Civil, Architectural, and Environmental Engineering, Univ. of Miami, 1251 Memorial Dr., Room MEB 325, Coral Gables, FL 33146. Email: d.arboleda@umiami.edu

[3]Professor, Dept. of Architecture, Built Environment, and Construction Engineering, Politecnico di Milano, Piazza Leonardo da Vinci 32, Milano 20133, Italy. Email: carlo.poggi@polimi.it

[4]Professor and Chair, Dept. of Civil, Architectural, and Environmental Engineering, Univ. of Miami, 1251 Memorial Dr., Room MEB 325, Coral Gables, FL 33146. ORCID: https://orcid.org/0000-0003-2678-9268. Email: nanni@miami.edu

Note. This manuscript was submitted on January 4, 2019; approved on June 5, 2019; published online on December 7, 2019. Discussion period open until May 7, 2020; separate discussions must be submitted for individual papers. This paper is part of the ***Journal of Composites for Construction***, © ASCE, ISSN 1090-0268.

Importance of Bond Testing

Several of the test methods used to characterize FRCM systems are adaptations of existing methods used in fiber-reinforced polymer (FRP) system investigations. Recent research studies have demonstrated that the performance of structural elements strengthened with FRP is related to the debonding strength of the FRP reinforcement from the substrate (Valluzzi et al. 2012; Colombi et al. 2014; Carozzi et al. 2015; CNR 2013). Debonding is a brittle failure mode not desirable for structural safety, which is mitigated by strength-reduction factors, thus making the bond strength quality and evaluation extremely important. Investigations have been carried on the debonding load and effective bond length of masonry or concrete elements strengthened with FRP laminates (Briccoli Bati et al. 2010; Aiello and Sciolti 2006; Capozucca 2010; Kwiecień 2012). Effective bond length is the length that, if exceeded, would not increase the force transferred between the FRP and the substrate. In those studies, the strain and stress distributions were generally recorded by means of resistance strain gauges located on the FRP surface. Different analytical models have been described by Capozucca (2010), Carrara and Freddi (2014), Colombi et al. (2014), D'Antino et al. (2015), Carozzi et al. (2015), Carloni and Focacci (2016), and Carozzi et al. (2016). The analytical models were proposed and validated through experimental data for the shear stress-slip behavior at the FRP/substrate interface. Due to the typical failure mode, the mechanical properties of the substrate play a significant role in the analysis of the bond behavior of the FRP reinforcement.

A case-specific analysis must be performed for FRCM reinforcement because it has different adhesion properties with the substrate due to the fact that its matrix is a mortar rather than an

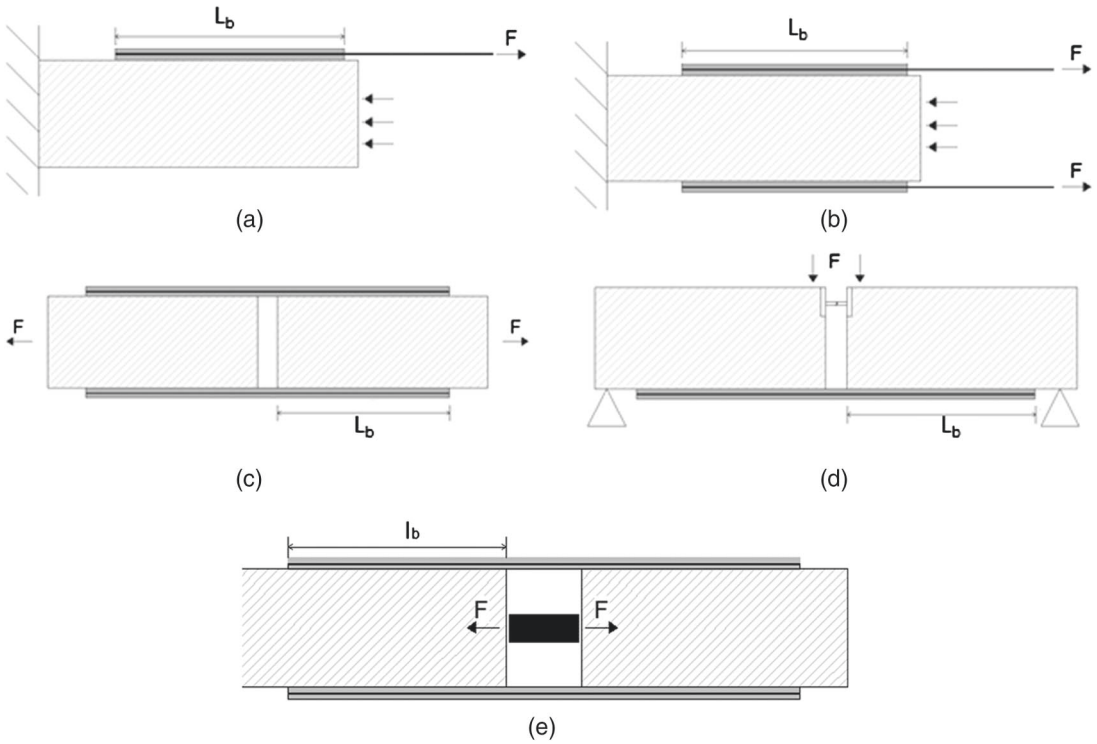

Fig. 1. Typical bond test setups: (a) single shear; (b) double-lap shear; (c) double-blocks shear; (d) hinged beam; and (e) double lap with two blocks.

organic resin. Moreover, the adhesion between the fabric and mortar and the friction among fibers within the yarns must also be carefully examined because the mortar particles do not fully penetrate all the fibers in the yarns. Thus, a yarn is not completely wetted and only the external fibers are bonded (or partially bonded) to the matrix, whereas the internal fibers provide only frictional bond. This phenomenon has been called telescopic failure mode and was studied by Peled et al. (2008) and Dvorkin et al. (2013).

Bond Test Setups

Test setups already implemented for FRP systems have been adopted to investigate the bond properties of FRCM materials. Commonly used bond test setups are single-shear, double-shear, and beam tests shown in Fig. 1, where L_b is the bond length (De Santis et al. 2017).

The push-pull shear setup type is based on the application of a direct tensile force (pull) to the reinforcement applied either on one side (single lap) [Fig. 1(a)] (D'Antino et al. 2014; Valluzzi et al. 2012; de Felice et al. 2014; D'Antino and Pellegrino 2014; Lu et al. 2005), or on the two opposite sides of the substrate block (double lap) [Fig. 1(b)] (D'Ambrisi et al. 2012; Valluzzi et al. 2012; Ceroni et al. 2014; Mostofinejad and Tabatabaei Kashani 2013; Malena and de Felice 2014; Carbone 2014; D'Ambrisi et al. 2013), while applying a force (push) on the block surface perpendicular to the reinforcement. Both of these setups present some challenges. The single shear could be influenced by eccentricity and misalignment of the fabric, which could skew the test results. In the double shear, it is important to ensure a homogeneous stress distribution on the two laps; moreover, once one of the two sides starts to fail, the system loses symmetry and alignment between the fabric and the axis of the testing machine.

Double-lap shear tests can be performed with a different configuration where the specimens are made from two different blocks that are bonded together by the reinforcement [Figs. 1(c and e)] (Carozzi et al. 2014). In the setup shown in Fig. 1(c), a steel plate and bar configuration inserted through the center of the blocks connects the specimen to the testing frame and generates the tensile load between the blocks, resulting in a symmetric load application. In the setup in Fig. 1(e), a jack is placed between the blocks to apply the load producing a different distribution of stresses. In both cases, the preparation and installation of the specimen is challenging, and thus impractical, because the goal is to ensure correct alignment between the two sides of the reinforcement.

Another test setup is the hinged beam test [Fig. 1(d)] (Mukhtar and Faysal 2018). In this configuration, the specimen is composed of two blocks that are connected on one side by the reinforcement and on the other side by a frictionless hinge. The beam formed by the two blocks is placed on two supports with the hinge on the compressive side and the reinforcement on the tension side, allowing for a four-point bending test. The tension in the reinforcement is a function of the bending moment at midspan. In this setup, the curvature of the specimen can induce compression stresses normal to the reinforcement–substrate interface, and the shear strength could appear higher than in pure shear loading conditions.

Debonding Behavior of FRCM Composites

For FRCM, when single-shear or double-shear test setups are used, the load is applied to the fabric only (not the full composite) and the following failure modes can be obtained (Fig. 2):

- Failure mode A: debonding with cohesive failure of the substrate. Although this failure is common for FRP systems, it is very uncommon for FRCM systems.
- Failure mode B: debonding at the interface between FRCM and substrate.
- Failure mode C: debonding at the FRCM fabric–matrix interface.
- Failure mode D: fabric slippage inside the mortar layer without visible cracks in the external mortar layer.

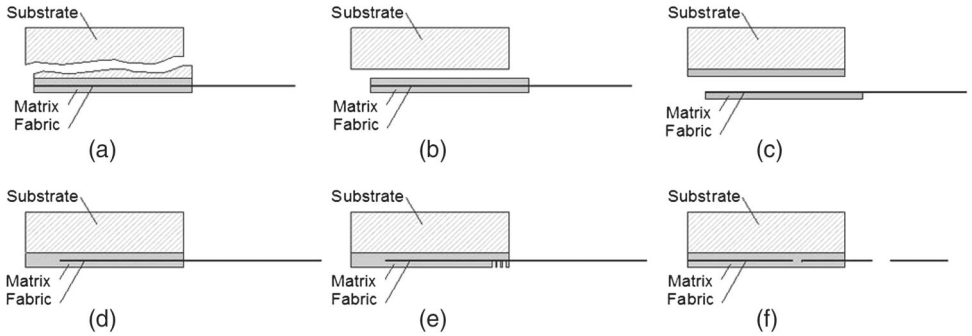

Fig. 2. FRCM bond failure modes: (a) debonding with cohesive failure of the substrate; (b) debonding at the matrix-to-substrate interface; (c) debonding at the fabric-to-matrix interface; (d) fabric slippage within the matrix; (e) fabric slippage within the matrix with cracking of the mortar; and (f) tensile failure of the fabric.

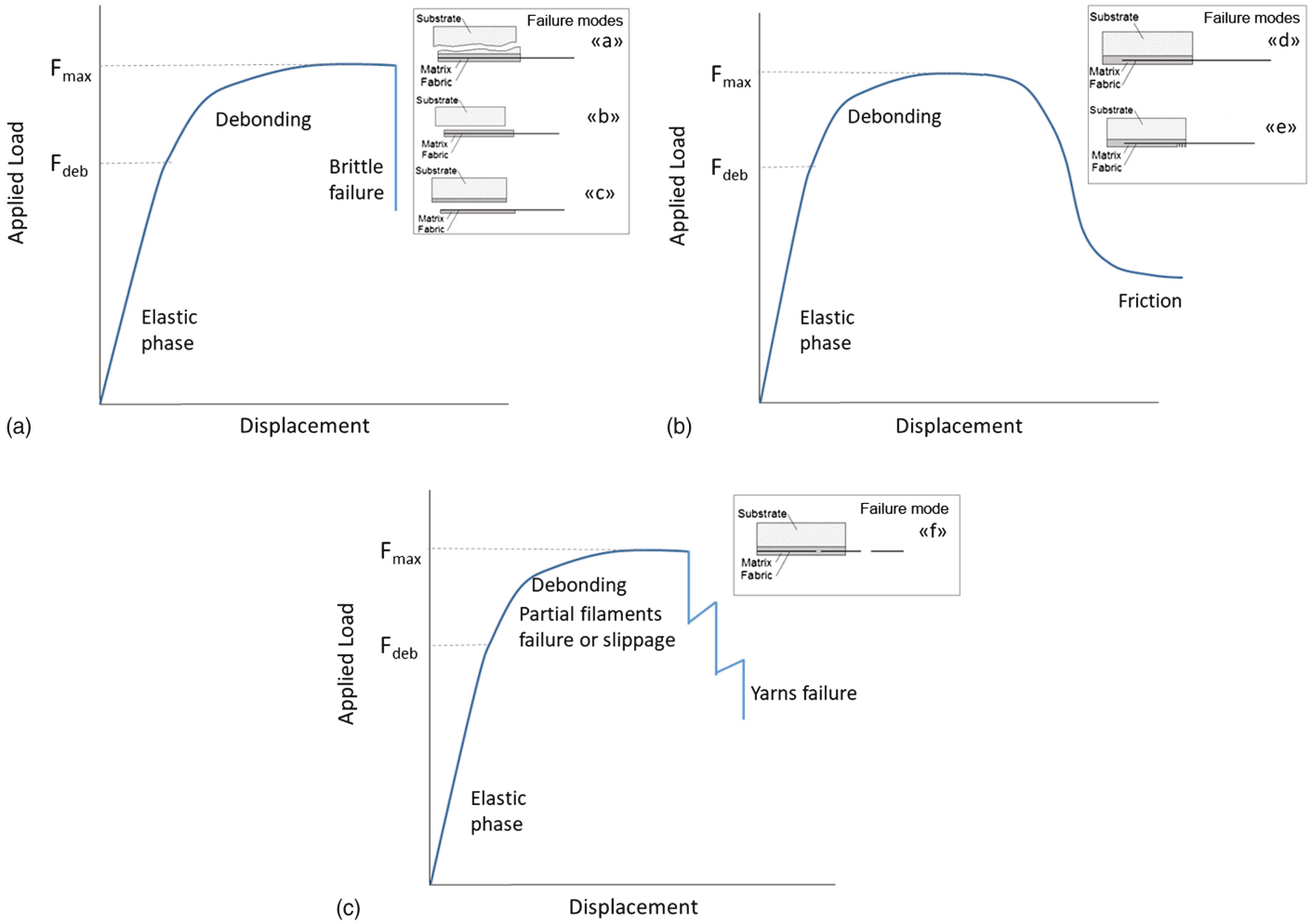

Fig. 3. Idealized load-displacement curves for different failure modes: (a) Failure modes A, B, and C; (b) Failure modes D and E; and (c) Failure mode F.

- Failure mode E: fabric slippage inside the mortar with visible cracks in the external mortar layer.
- Failure mode F: tensile failure of the fabric in the bonded or unbonded part.

The failure mode is a function of several factors, namely (1) mechanical properties of the mortar and fabric; (2) geometry of the fabric and the yarn area; (3) bond length; (4) adhesion properties between mortar and substrate and mortar and fabric; (5) friction between fibers; and (6) any partial external impregnation of the fibers.

Fig. 3 shows the idealized load-displacement curves related to the possible failure modes for specimens with a bond length longer than the effective bond length. This bond length is generally defined as the one that ensures a complete stress distribution through the length of the reinforcement (Carozzi et al. 2016). The debonding phase during the test is supposed to be evident, and the load is

gradually transferred along the length of the composite system. Obviously, this is an assumption that is not always verified during the experimental tests, and it is related to the rate of load application and how the load is controlled.

For Failure modes A–C described in Fig. 2, the curve is elastic until a debonding load (F_{deb}) is reached. After that, the slope decreases due to the propagation of debonding, up to the failure caused by the complete detachment. This behavior is similar to the one obtained with FRP systems (Carozzi et al. 2015), which present a typical failure mode characterized by the debonding with cohesive failure of the substrate as depicted in Fig. 3(a).

For Failure modes D and E, which are due to fabric slippage, three phases can be identified [Fig. 3(b)]. The elastic phase is up to the debonding load where the load is transferred from the fabric to the mortar and substrate. After this phase, the stress increase causes debonding between fabric and mortar. If the bond length is greater than the effective length (Carozzi et al. 2016), the slope of the load-displacement curve decreases. When the maximum stress is transferred to the entire bond length, the load decreases with a slope related to the adhesion properties between the mortar and fabric. The last phase, characterized by a constant load (F_{fr}), is due to frictional resistance among fibers or between fibers and mortar matrix.

For Failure mode F, the curve [Fig. 3(c)] shows a series of drops after the maximum load due to the progressive failure of the yarns. A debonding failure could be also result in the progressive breakage of the filaments in the yarns.

The theoretical analysis of the bond characteristics of FRCM reinforcement systems are different with respect to the ones developed for FRP materials. This is due to the failure modes, which are related to fiber slippage and breakage at the fabric–mortar interface, and less commonly due to debonding of the composite from the substrate. From a safety standpoint, fiber slippage exhibits some pseudoductility, which is a more favorable type of failure.

Recently, research studies were conducted to investigate the bond performance of FRCM systems. Banholzer (2004) and Banholzer et al. (2006) investigated the pull-out behavior of yarns embedded in a cementitious matrix and of single fibers in a yarn. They proposed a model that provides a simple and straightforward analytical method to evaluate the prevailing bond characteristics of a composite by means of a bond stress versus slip relation using experimental data from pull-out tests. D'Ambrisi et al. (2012) studied a local bond-slip relation calibrated on experimental results; this relation was implemented in the modeling of structural behavior of reinforced concrete elements strengthened with FRCM and was used to calculate the effective bond length and the force that could be transferred between reinforcement and substrate. D'Antino (2014) studied a fracture-mechanics approach to analyze the stress and strain distribution between mortar and fabric. Carozzi et al. (2016) proposed a cohesive interface crack model based on a trilinear bond-displacement behavior at the textile–matrix interface. Malena and de Felice (2014) presented a model to investigate the shear and normal stress distributions in FRCM composites applied over a curved substrate.

Experimental Program

For this study, six FRCM systems were investigated using push-pull single-shear and double-shear test setups [Figs. 1(a and b)]. These setups are easier to implement and more economical and reliable than the double blocks or hinged beam tests. The single-lap configuration was selected to guarantee a homogeneous stress distribution in the fabric. Conversely, the double-lap setup avoids eccentricity issues related to the single-shear configuration. The discussion of the experimental results also involves a comparison between the results obtained with these two different configurations. Different substrates and specimen geometries were considered. This work is part of a larger experimental program (Carozzi and Poggi 2015). The results obtained with the single-lap configuration were compared with similar tests performed on different FRCM materials in a round-robin project organized by Réunion Internationale des Laboratoires et Experts des Matériaux, systèmes de construction et ouvrages (RILEM) TC-250 composites for sustainable strengthening of masonry (CSM) and described by Caggegi et al. (2017), Carozzi et al. (2017), and Leone et al. (2017).

Materials

Six FRCM systems were studied; each fabric material was applied with its specific mortar in order to guarantee the optimum adhesion between fabric and matrix and to have the correct granulometry. The fabric materials used were as follows:

- polyparaphenylene benzobisoxazole (PBO) balanced fabric made of 15-mm spaced yarns with a nominal equivalent thickness equal to 0.014 mm;
- carbon (C) fiber balanced fabric with yarns disposed in two orthogonal directions at a nominal spacing of 10 mm and nominal equivalent thickness of 0.047 mm;
- coated carbon (cC) unbalanced fabric with clear space between yarns equal to 7 and 19 mm in weft and warp directions, respectively, where the equivalent thickness in the warp direction is 0.22 mm;
- glass (G) balanced fabric with a nominal equivalent thickness equal to 0.036 mm and a space between the yarns equal to about 6 mm;
- glass with a coating of styrene butadiene rubber (cG) unbalanced fabric with clear space between yarns equal to 17 and 12 mm in weft and warp directions, where the equivalent thickness in the warp direction is 0.047 mm; and
- PBO-glass (PBO-G) balanced fabric composed of PBO and glass yarns with a free space between yarns equal to 14 mm and a nominal equivalent thickness of 0.0064 mm.

For the fabrics with coated yarns, the coating is only an external treatment that does not impregnate the internal fibers of the yarn. Tensile tests were performed according to EN ISO 10618 (ISO 2005) on a single yarn and/or on a fabric strip of width equal to 40 or 50 mm in the warp direction. Table 1 summarizes the average results. For the PBO-G fabric, only the PBO yarns are considered because the failure is controlled by the PBO having the higher ultimate strain. (Carozzi et al. 2015; Arboleda et al. 2015). The cross-section area of one yarn (A_f) is also reported in Table 1. The tests were performed on dry yarns without any impregnation with resin; in some cases, the failure was caused by the rupture of some single filaments with slippage between the remaining filaments. For this reason, the stress reached at failure could be lower than the fiber strength.

Table 2 presents the mechanical properties of the matrices and the corresponding standard test methods. Some of the values were verified by the authors, whereas others were taken from the technical data sheets provided by the respective manufacturer. All the matrices were cementitious mortars except the matrix used for glass fabric (G), which was a lime mortar.

Specimen Geometry

A total of 72 tests were performed. Different substrate materials consisting of solid clay bricks and concrete were used based on the target repair application of the FRCM systems. PBO-FRCM, PBO-G-FRCM, C-FRCM, and G-FRCM were applied on clay

Table 1. Mechanical properties of fabric strips

Fabric type	Number of yarns	A_f (mm^2)	Number of tests	Avg. stress at failure (MPa)	COV (%)	Elastic modulus (GPa)	COV (%)
PBO	1	0.22	6	3,280	2.6	216	20.8
Carbon (C)	1	0.47	3	1,944	14.9	203	9.8
	4	1.88	3	1,913	10.4	—	—
Coated carbon (cC)	1	2.68	3	1,320	9.2	263	11.2
Glass (G)	1	0.24	4	832	11.4	81	4.3
Coated glass (cG)	1	0.90	5	1,233	2.7	56	30.5
	3	2.70	5	1,121	1.3	—	—
PBO-G	2 PBO, 1 glass	0.42 (only PBO)	3	2,996	11.9	—	—

Note: COV = coefficient of variation.

Table 2. Mechanical properties of the matrix

Fabric type	Compressive test[a] (MPa) Strength	COV (%)	Flexural strength[a] (MPa) Strength	COV (%)	Elastic modulus[b] (GPa)
PBO	20 (ds)	—	>2 (ds)	—	>6 (ds)
Carbon (C)	24 (5)	2.5	3.5 (ds)	—	>7 (ds)
Coated carbon (cC)	>45 (ds)	—	7 (ds)	—	7 (ds)
Glass (G)	7.48 (6)	1.3	3.16 (3)	6.45	6.1 (3)
Coated glass (cG)	27 (7)	4.1	8.4 (14)	13.15	8 (ds)
PBO-G	20 (ds)	—	3.5 (ds)	—	7.5 (ds)

Note: Parentheses indicate the number of tested coupons or source of data; ds = data sheet.
[a]Tested according to CEN (2007).
[b]Tested according to ISO (2011).

bricks with a compressive strength of 20.8 MPa. The cG-FRCM was applied on clay bricks with a compressive strength of 68.8 MPa (Carozzi et al. 2014). The cC–FRCM was applied on a concrete prism substrate with a compressive strength of 31 MPa.

Different FRCM geometries were considered (Table 3). For each configuration, only a single layer of fabric was applied. All the samples were reinforced with a double-lap configuration except the ones with a bond length of 260 mm, which were single lap. The specific steps taken are as follows:

- PBO, PBO-G, and G-FRCM were bonded to a substrate block composed of a variable number of bricks and mortar joints (from three to five) depending on the reinforcement bond length.
- C-FRCM was bonded both to a block composed of a single brick and to a masonry block composed of a variable number of bricks and mortar joints (from three to five) depending on the reinforcement bond length.
- cC-FRCM was bonded to a $100 \times 100 \times 300$ mm concrete prism;
- cG-FRCM was bonded to a single clay brick and to masonry blocks composed of five clay bricks.

Different bond lengths and widths were considered to investigate the effect of these parameters on the debonding strength and failure mode. FRCM was installed after the 28-day curing period of the concrete substrate or the mortar used for the masonry blocks. In order to avoid boundary effects, a 20-mm gap was left on the substrate on the pull side of the specimens. The total thickness of the FRCM matrix was approximately 10 mm, and the fabric was applied between two layers of mortar matrix, with particular attention to ensure correct alignment of the yarns. For the double-lap configuration, the fabric was a continuous sheet that after being applied to one side of the specimen, was then looped (like a suspender) and applied to the other side of the specimen. The specimens' geometry is shown in Fig. 4. Testing was performed after the 28-day curing period of the FRCM matrix.

Test Setups

Two similar test setups were used to implement the pull-push single-shear and double-shear tests with uniaxial test frames (Fig. 5). For both double-lap test configurations, a supporting metal cage was implemented at the bottom grip of the frame to keep the specimen in place, and a steel cylinder with a diameter equal to the distance between the two fabric strips was used at the top grip to apply the tensile load equally to both sides of the specimen. Spherical or multiple-degree-of-freedom joints were used to ensure the correct position of the specimen and avoid possible misalignments of the applied load. Two Teflon polytetrafluorethylene sheets were placed between the cylinder and fabric in order to minimize friction. The stiffness of the setup was verified, and its deformability was considered negligible (Carozzi and Poggi 2015). For the

Table 3. Geometry of shear FRCM tests

Reinforcement type	Bond length (mm)	Bond length (mm)	Bond length (mm)	Bond length (mm)	Reinforcement width (mm)	Substrate[a]
PBO-FRCM	100 (3)	150 (3)	260 (5)	—	85 (7)	Three solid clay bricks
					100 (8)	
C-FRCM	100 (3)	150 (4)	200 (5)	—	100 (10)	Three/four solid bricks
	50 (5)	100 (5)	150 (5)	—	70 (7)	Single solid clay brick
cC-FRCM	150 (5)	200 (5)	250 (5)	—	50 (3)	Concrete
G-FRCM	200 (5)	—	—	—	100 (12)	Four solid clay bricks
cG-FRCM	50 (5)	100 (5)	150 (5)	260 (4)	50 (3)	One/five solid clay bricks
					100 (5)	
PBO-G-FRCM	—	100 (3)	150 (4)	200 (5)	100 (7)	Three/four solid bricks

Note: Parentheses indicate number of samples; brackets indicate number of yarns per side.
[a]Number of bricks is dictated by bond length.

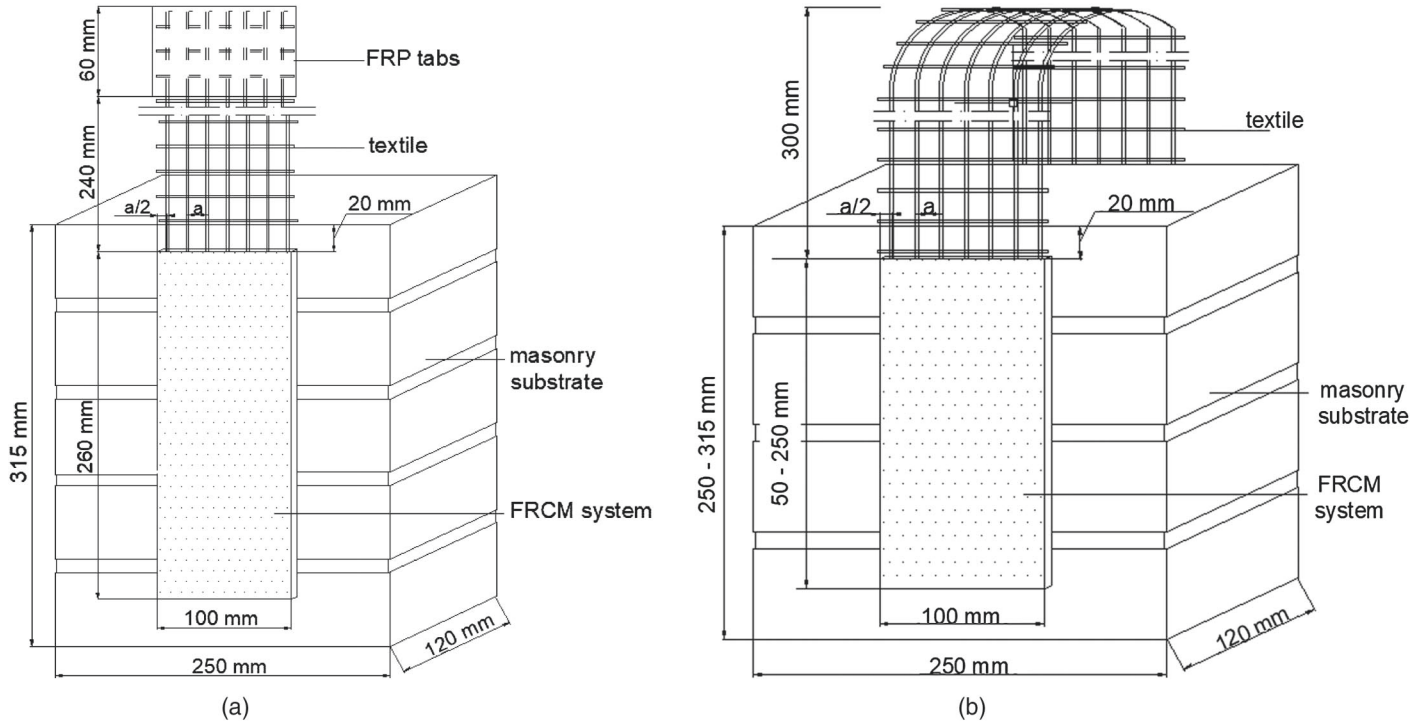

Fig. 4. Samples' geometry: (a) single lap; and (b) double lap (millimeters).

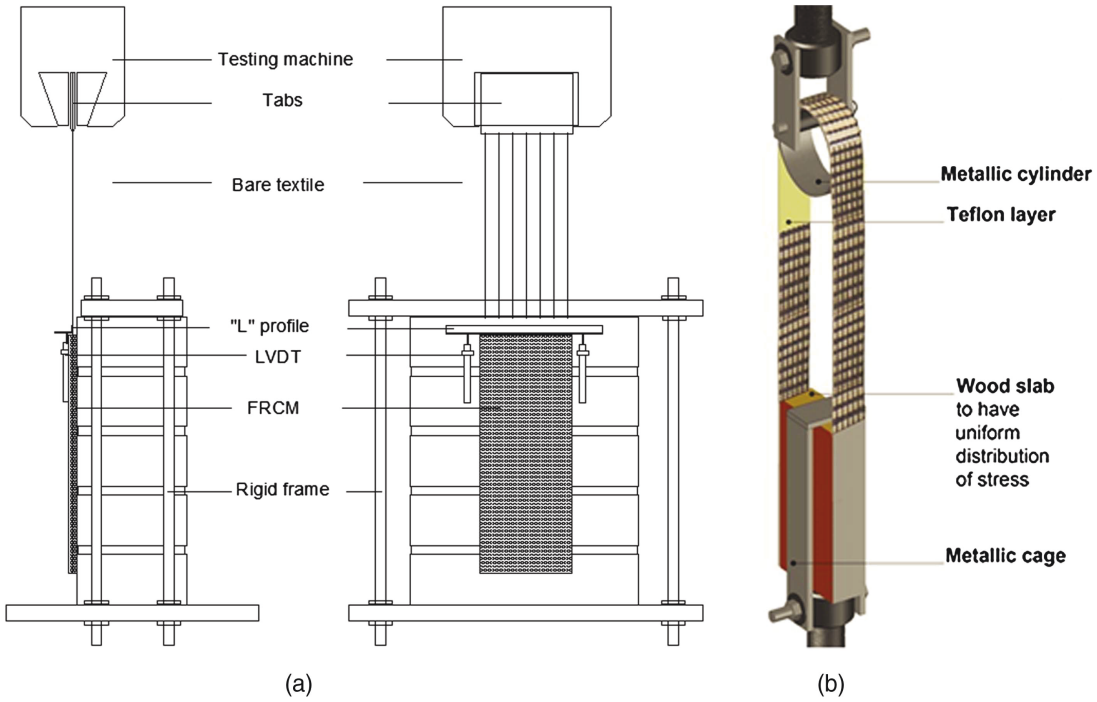

Fig. 5. Test setups: (a) single lap; and (b) double lap.

single-lap shear tests, the FRCM system was applied on a surface of the masonry substrate, and a portion of fabric was left unbonded with a length equal to about 300 mm. A steel frame similar to the one previously described was used to fix the sample in the testing machine and to guarantee the alignment between the FRCM system and the longitudinal axial of the machine. At the end of the unbonded fabric, two FRP tabs were glued with epoxy resin. This part was inserted in two bolted metal plates connected to the testing machine with a spherical joint, in order to distribute the stresses.

The slips between fabric and matrix were recorded with two (for single-lap setup) or four (for double-lap setup) LVDTs. The instruments were located on the substrate and reacted off an L-shape profile glued to the bare fabric in the area adjacent to the mortar.

Table 4. Experimental results

Fabric	Bond length (mm)	Bond width (mm)	Initial stiffness (N/mm)		Failure load (kN)[a]		Stress in yarns at failure (MPa)[b]	Load/width (N/mm)[b]	Fabric stress/fabric strength (%)	Failure mode	Failure mechanism
			Avg.	Standard deviation	Avg.	Standard deviation					
PBO-FRCM	100^{DL}	85	1,042	25	7.8	0.7	2,542	46.1	80	D and F	Fiber slippage and partial fiber rupture in weft and warp directions
	150^{DL}	85	739	155	8.1	1.1	2,617	44.5	77		
	260^{SL}	100	802	48	4.1	0.3	2,412	39.4	69		
C-FRCM	100^{DL}	100	1,703	153	10.2	0.3	1,084	46.3	57	D and F	Partial fiber rupture in weft and warp directions and subsequent slippage of the fabric
	150^{DL}	100	1,504	289	10.4	0.6	1,108	47.4	59		
	200^{DL}	100	1,576	97	10.9	1.1	1,159	49.5	65		
	50^{DL}	70	1,141	186	4.2	0.4	644	30.3	37	D	Fabric slippage
	100^{DL}	70	1,953	197	6.0	0.2	911	42.9	53	D	Fabric slippage
	150^{DL}	70	1,741	781	8.1	0.5	1,223	57.5	70	D and F	Slippage and rupture of some fibers
cC-FRCM	150^{DL}	50	3,677	608	16.0	1.7	1,068	160.3	82	F	Fabric rupture
	200^{DL}	50	3,583	170	18.8	1.2	1,253	188.0	96	F	Fabric rupture
	250^{DL}	50	3,670	172	21.4	2.1	1,428	214.3	110	F	Fabric rupture
cG-FRCM	50^{DL}	50	697	64	1.1	0.2	196	10.6	16	D	Fabric slippage
	100^{DL}	50	644	17	2.6	0.2	487	26.3	39	D and F	Slippage and subsequent partial fabric rupture
	150^{DL}	50	670	64	4.1	0.6	751	40.6	61	F	Fabric rupture and slippage
	260^{SL}	100	1,012	24	3.1	0.2	691	31.1	56		
G-FRCM	200^{DL}	100	563	35	2.1	0.4	738	5.31	89	E and F	Mortar cracking, fabric slippage, and rupture
PBO-G-FRCM	100^{DL}	100	680	72	4.3	0.4	1,776	21.3	59	F	Complete rupture of glass fibers and partial rupture of PBO fibers
	150^{DL}	100	701	38	4.6	0.8	1,933	23.2	66		
	200^{DL}	100	722	48	5.4	0.3	2,253	27.1	83		

Note: SL = single lap; and DL = double lap.

[a]Total load applied to the specimen.

[b]Theoretical stress and load/width assuming a uniform stress distribution in the yarns.

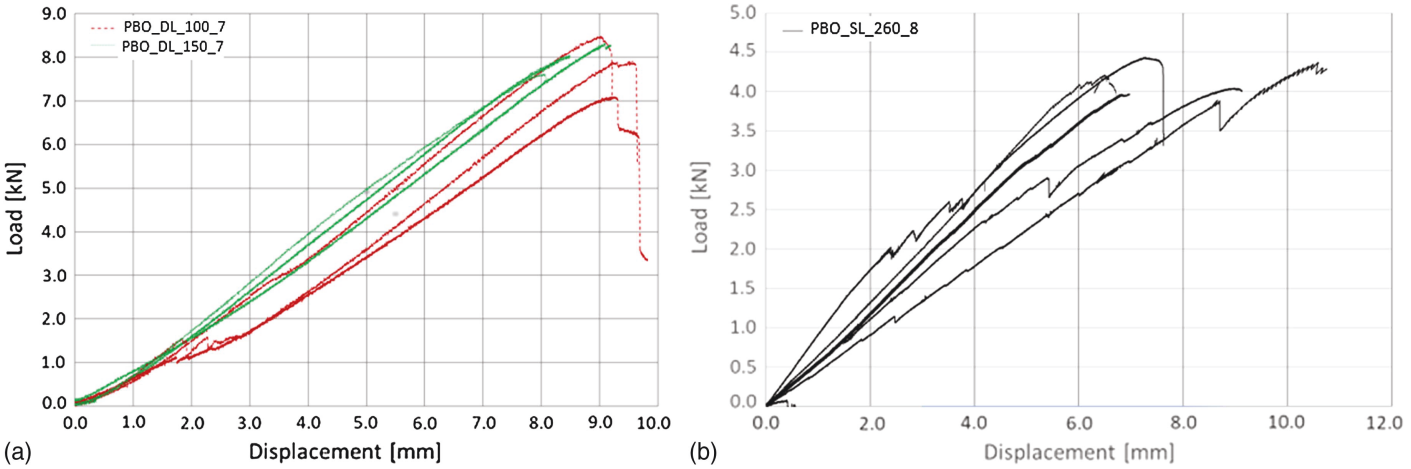

Fig. 6. Load-displacement curves: (a) PBO_DL_100/150_7; and (b) PBO_SL_260_8.

Experimental Results

For all specimens, the applied load was monitored while the relative displacement of the grips of the testing machine was recorded, subtracting the elongation of the unbonded fabric. Table 4 summarizes the results obtained, which include (1) initial stiffness corresponding to the first linear phase of the graph; (2) load at failure; (3) theoretical stress in the yarn assuming a uniform stress distribution; (4) load per unit width; (5) effectiveness ratio, which is the ratio of stress in yarns at failure and the fabric strength reported in Table 1; and (6) failure mode as it relates to Fig. 2.

The samples are named Material_SL/DL_x_y where SL or DL indicates the single-lap or double-lap configuration, x is the bond length (mm), and y represents the number of yarns in the width direction.

An analysis of the experimental curves and failure modes follows noting that the load-displacement curves are not comparable with the idealized curve [Fig. 3(c)] because the experimental tests were conducted under displacement control of the test frame and not by the slip between fabric and mortar matrix.

Tests on PBO-FRCM

The tests with PBO-FRCM samples did not show a significant difference between different bond lengths, both on the failure mechanism and maximum load. Due to the higher bond length, it was expected that the samples tested with the single-lap setup will give a higher maximum stress. Probably, this was not verified due to a nonhomogeneous stresses distribution in the width of the sample and problems in fabric gripping. Fig. 6 shows the load-displacement curves. The failure was not abrupt with sudden breaking of all the fibers, but rather a progressive failure of the fibers and slippage between mortar and fabric (Fig. 7). In the tests performed with the single-lap setup, the slip between fabric and mortar was measured with two LVDTs, and the average slip corresponding to the maximum load was 1.04 mm.

Tests on C-FRCM

The tests with C-FRCM were performed on single clay bricks and on blocks made of three solid clay bricks; the bond lengths investigated were 50, 100, 150, and 200 mm. The shorter bond lengths were investigated at 60- and 100-mm widths where the smaller-width specimens experienced slippage of the fabric at loads lower than the tensile strength of the carbon fibers. The wider specimens experienced both fiber breakage and slippage. The longer bond length had a partial fiber failure in weft and warp directions and subsequent slippage of the fabric. None of the specimens experienced debonding of the FRCM system from the substrate. Fig. 8 shows the load-displacement curves for samples with a bond width equal to 100 mm for the different bond lengths. The results show an increment in the maximum stress from 644 MPa for the samples with a bond length equal to 50 mm to a maximum stress equal to 1,223 MPa for the samples with a bond length equal to 150 mm. Furthermore, samples with a lower width presented higher stresses

Fig. 7. Failure modes: (a) PBO-FRCM; (b) C-FRCM; (c) cCFRCM; (d) c-FRCM; (e) G-FRCM; and (f) PBO-G-FRCM.

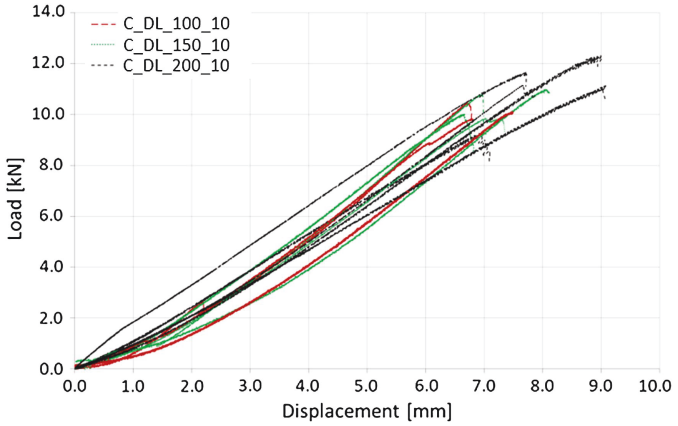

Fig. 8. Load-displacement curves for C_DL_100/150/200_10.

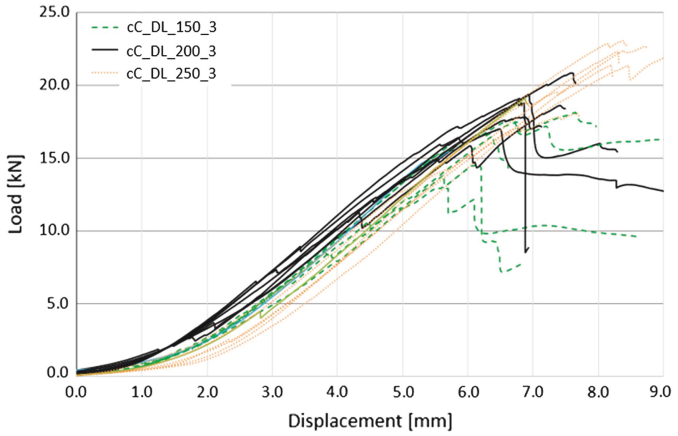

Fig. 9. Load-displacement curves and failure mode for cC-FRCM.

for the same bond length. This is probably due to a lower rotation of the fabric in the transversal direction and consequently more homogeneous stresses distribution in the yarns. Moreover, the substrate of these samples consisted of only one block, so possible problems in the alignment between the bricks were avoided.

Tests on cC-FRCM

The tests with cC-FRCM were performed on concrete prisms and with bond lengths of 150, 200, and 250 mm. All the tests resulted in linear behavior of the material up to partial rupture of the fibers. The failure load increased with the bond length. The shorter reinforcement length had the highest variability in both initial stiffness and failure load. Fig. 9 shows the load-displacement curves for the three bond lengths.

Tests on cG-FRCM

cG-FRCM was applied on single clay bricks with a bond length equal to 50, 100, and 150 mm. Fig. 10 shows the load-displacement curves for the different bond lengths. The failure load increased with the bond length. Shorter reinforcement lengths (50 and 100 mm) showed fabric slippage at loads smaller than the tensile strength of the glass fibers. For the longer bond lengths, a fabric failure was experienced with an average maximum load of 4.06 kN. None of the specimens experienced debonding of the FRCM system from the substrate.

The reinforcement was tested also with a bond length equal to 260 mm. In this case, the single-lap setup was used, and the cG-FRCM system was applied on a substrate composed of five bricks. The maximum load was not much higher than that for specimens with bond length equal to 150 mm. Even if some problems in the stresses distribution should be considered (as described for C-FRCM samples), it is possible that the effective bond length was reached because the collapse was due to fabric failure located near the bonded area. In the tests performed with the single-lap setup, the slip between fabric and mortar was measured with two LVDTs, and the average slip corresponding to the maximum load was 1.2 mm.

Tests on G-FRCM

G-FRCM, made with glass fabric and lime-based mortar, was applied on blocks made by four bricks with a bond length of 200 mm. The failure mode was characterized by longitudinal and transversal cracking of the mortar, slippage between fabric and mortar, and debonding of the external layer of mortar from the fabric. In a few tests, some longitudinal cracks were observed between FRCM and substrate.

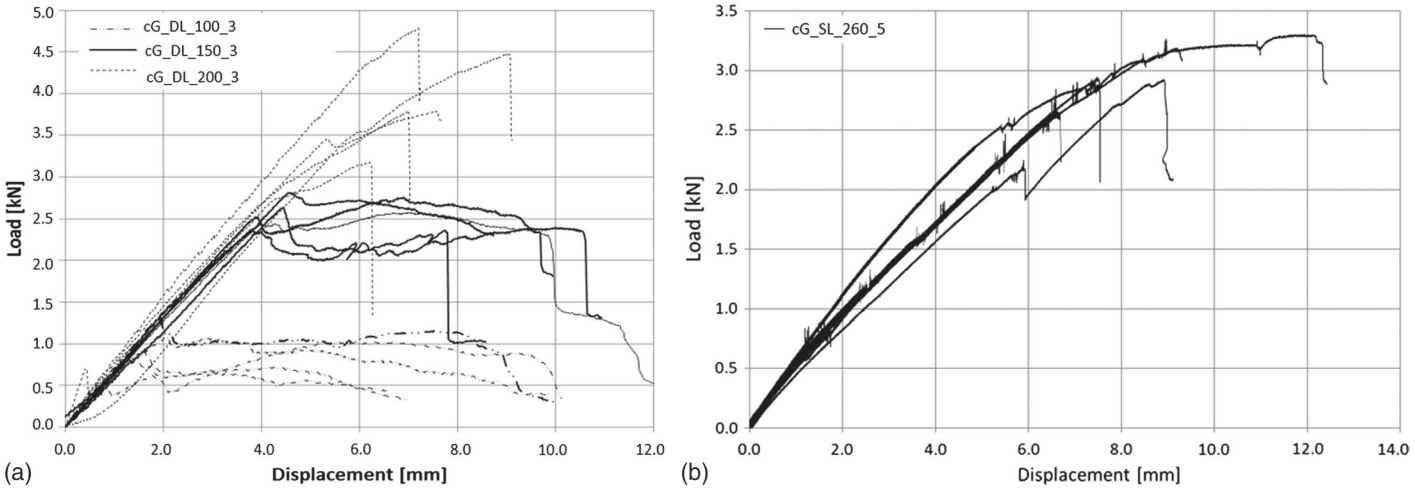

Fig. 10. Load-displacement curves: (a) cG_DL_50/100/150_50; and (b) cG_SL_260_5.

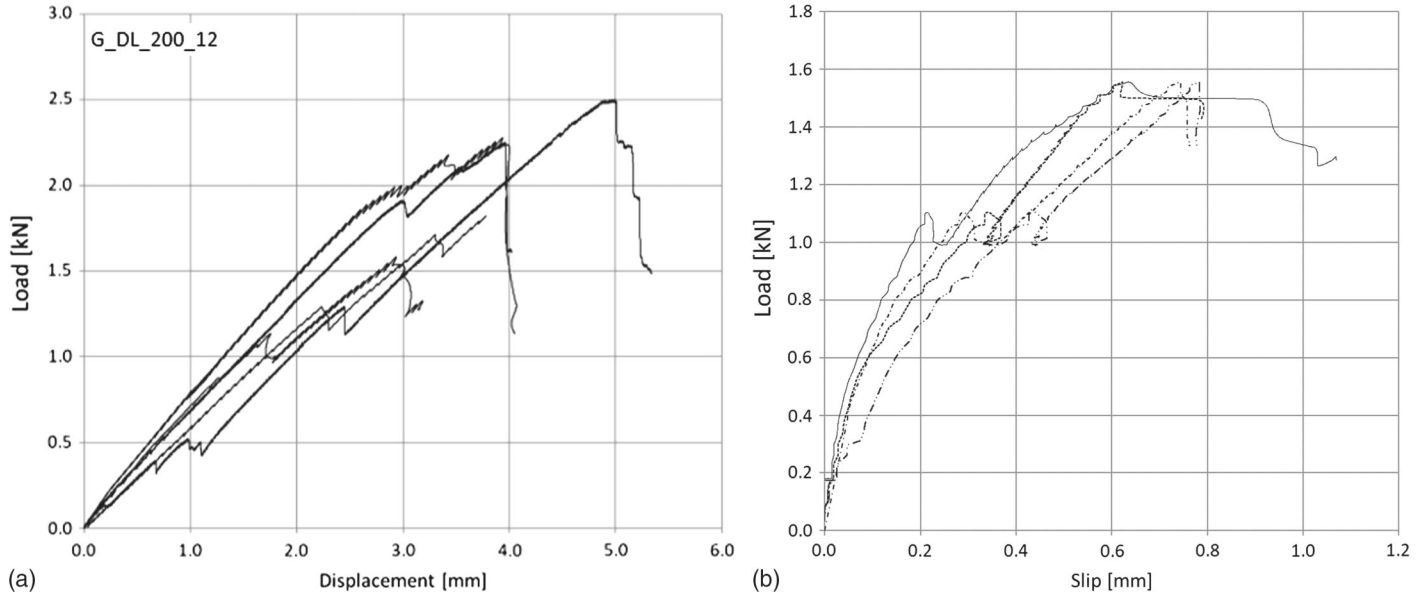

Fig. 11. G_DL_200_12 samples: (a) load-displacement curves; and (b) load-slip curves for one test (four LVDTs).

Four LVDTs (two per side) were installed to measure the slip between the fabric and the mortar (Fig. 4) and to monitor load distribution and rotation of the fabric during the test. Fig. 11 shows the load-displacement curves and load-slip curves of one test, where each curve represents the data recorded by the correspondent LVDT. There was a first elastic phase in which the four curves are parallel. Then, at a load equal to about 1.1 kN, there was a drop in the load with slip increment due to the cracking of the mortar both with a progressive detachment at textile–mortar interface and transversal cracks. After that, a second phase with a lower stiffness occurred, possibly due to fiber slippage. The curves recorded by the four LVDTs showed that in the first phase, one instrument measured higher displacement, probably due to load assessment. After that, the slopes are quite parallel, and the slip measured at the peak load was equal to about 0.7 mm. Fig. 7 also shows a typical failure.

The lime mortar used in this system presents lower mechanical properties with respect to the other mortars, which often contain polymers. The advantages of this system are related to the reversibility and compatibility with the masonry substrate, which could be evaluated by the chemical properties and analysis of the coefficient of vapor permeability. For this reason, this system has useful applications in historical restoration, and it is preferred for Cultural Heritage conservation.

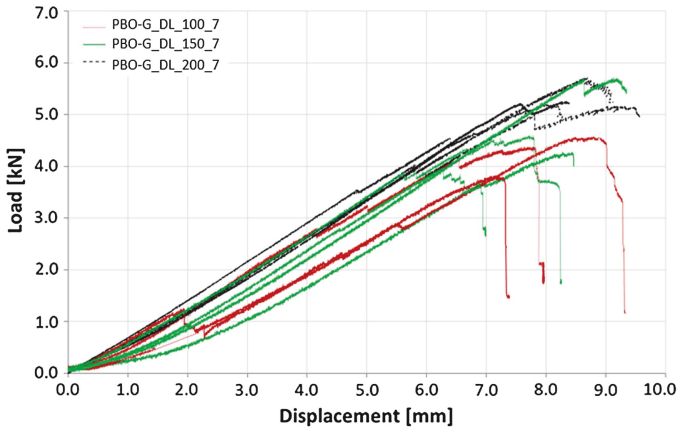

Fig. 12. Load-displacement curves for PBO-G-FRCM.

Tests on PBO-G-FRCM

The tests on PBO-G-FRCM specimens did not point to an influence of the bond length on the failure mechanism. The damage progression was first by breakage of the glass fibers at a relatively low load and then a gradual failure of the PBO fibers in the weft and warp.

The increment of the bond length caused an evident increment in the maximum stress reached that varies from 1,777 MPa for a bond length equal to 100 mm to 2,254 MPa for a bond length of 200 mm.

Fig. 12 shows the load-displacement curves for the different bond length analyzed. All the tests were performed with the double-lap configuration, and the maximum stress reported in Table 4 refers only to the cross-section area of the PBO fabric.

Discussion of Experimental Results

Fig. 13 shows a comparison among the stress-displacement envelopes for each system with the higher bond length. In particular, a bond length of 260 mm was used for the systems with PBO and cG fibers, a length equal to 250 mm was used for the cC-FRCM system, and the PBO-G, carbon, and glass fibers had a bond length equal to 200 mm.

PBO fabric is characterized by the better bond properties; the maximum stress reached with PBO-FRCM systems is about 55% higher than that of C-FRCM. The behavior of PBO-FRCM and PBO-G-FRCM is quite similar because the stresses on the PBO-G textile are computed also with respect to the PBO fibers. The cC-FRCM presents higher stiffness and maximum stresses with respect to the C-FRCM material, probably due to the presence of the coating, which increases the adhesion properties between fabric and matrix.

In the case of glass fibers, those with coating, cG-FRCM, present better behavior than G-FRCM. Moreover, G-FRCM has a very low strength due to the mechanical properties of the lime

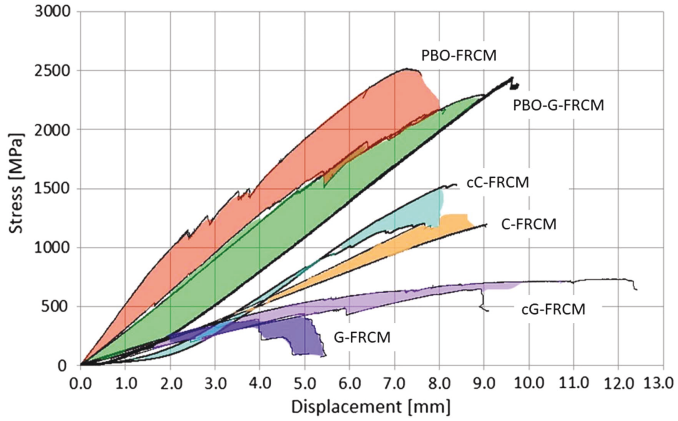

Fig. 13. Comparison between experimental results obtained for different FRCM materials.

mortar; in fact, the failure mode is characterized not only by the slippage of the fabric but also by the cracking and debonding of the mortar.

From the experimental results, it is possible to analyze the effective bond length of the FRCM reinforcement systems. In FRP materials, when the bond length is longer than the effective one, no load increment is obtained. On the opposite, in FRCM materials, the load increases linearly with a lower stiffness. This phenomenon, as depicted in Fig. 14(a), is due to the contribution of friction phenomena between the textile fibers and the mortar, which influences the shear stresses along the bond length. When debonding between fibers and matrix onsets, the shear stresses in the debonded part are not equal to zero, but a constant frictional stress develops and produces a load increment. The effective bond length is influenced by the materials' properties, and in particular by the bond behavior between matrix and fabric. An analytical method to calibrate the interfacial material law on a FRCM material and to estimate the effective bond length has been described by Focacci et al. (2017).

Fig. 14(b) shows an analysis of the stress increment as function of the bond length increment for different FRCM materials. Tests performed with different test setups (single and double laps) and with different bond widths are included in order to have a larger database.

For cG-FRCM systems, the stress increment up to a bond length of 150 mm is evident; no stress increment could be found if the bond length increases up to 260 mm. So the effective bond length for cG-FRCM could be considered equal to 150 mm.

The C-FRCM system shows a low stress increment up to a bond length of 200 mm. In contrast, the cC-FRCM system showed a continue increment from 100 to 250 mm. The effective bond length seems to be higher than this value; therefore, more experimental tests with longer bond lengths would be useful.

PBO-FRCM and PBO-G-FRCM seem to present an effective bond length higher than 200–260 mm, probably because the better adhesion properties between PBO yarns and matrix cause a higher contribution of friction and a consequent increment of the stresses.

Proposal for Inclusion in Guidelines and Acceptance Procedures

On the basis of the series of experiments performed, the following steps are proposed as a testing procedure for characterization of FRCM bond properties.

Specimen Geometry and Preparation

Regarding specimen geometry and preparation, it is suggested that the following factors be considered:

- The substrate block may be a concrete or a masonry prism (a number of bricks between three and six is suggested). In particular, the latter configuration may be used to investigate larger bond lengths and the influence of mortar joints.
- Surface preparation is important because it can influence the adhesion between the internal mortar layer and substrate.
- The surface of the substrate must be in a saturated surface dry condition before FRCM application in order to avoid excessive water absorption from the mortar.
- The reinforcement must be located at some distance (20–30 mm) from the upper edge of the substrate and from the side edges to avoid stress concentrations in the extremities of the substrate.
- A bond length of at least 250 mm is suggested. If a longer bond length is used, an increment in the maximum load after debonding due to friction may occur (D'Antino et al. 2015; Carozzi et al. 2016).
- The width of the mortar matrix must be equal to an integer multiple of the spacing between the fabric yarns in order to ensure a proper stress distribution between mortar and fabric.

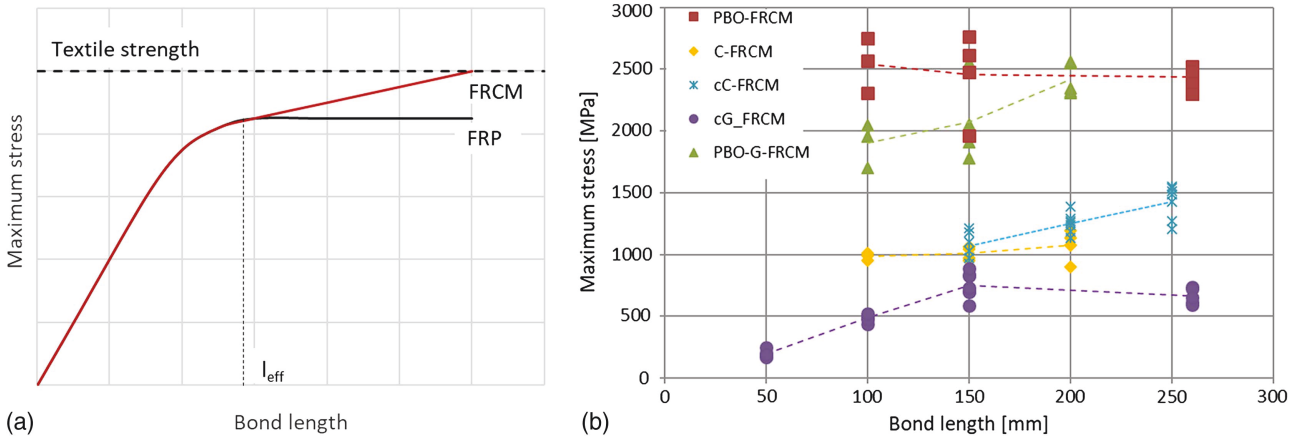

Fig. 14. Analysis of the effect of the bond length on the maximum stress: (a) theoretical behavior; and (b) experimental results.

- The thickness of the FRCM material must be similar to the one used in the strengthening application (typically 10 mm for a single layer).
- Proper alignment between the fabric and the substrate must be ensured.
- Curing shall last at least 28 days or as indicated by the manufacturer. In the curing phase, it is necessary to ensure adequate relative humidity (RH) conditions in order to prevent the development of differential shrinkages, which would cause cracking in the matrix. Before testing, the specimen should be stored in standard laboratory conditions (20°C–25°C and 50%–60% RH) for at least 7 days.

Test Setup

Both single-lap and double-lap configurations are acceptable. For a single lap, the following should be considered:

- The sample must be located in a steel frame that is stiff enough to avoid rotations and distortions.
- The location of the specimen must guarantee the alignment between the upper plate of the supporting frame and the fabric strip in order to have pure shear stress at the substrate to matrix interface.
- The free end of the strip should be clamped to the testing machine using tabs in FRP or aluminum material in order to ensure a homogeneous distribution of the stresses and avoid slippage. A minimum length of 60 mm is suggested for the tabs with a minimum thickness of 2 mm (tensile tests have demonstrated that a length of 60 mm is enough to ensure that no slippage from the tabs occurs).

For the double-lap, the following should be ensured:

- The sample must be located in a test frame stiff enough to avoid rotations and distortions.
- Alignment between the specimen and the loaded end must be ensured in order to avoid bending stresses at the reinforcement-to-substrate interface.
- To obtain the best homogeneous stress distribution in the two faces of the sample, the fabric must be placed around a steel cylinder with a diameter equal to the distance between the two fabric strips.
- Friction between the fabric and steel cylinder grip must be minimized. A roller device working as cylindrical hinges or two Teflon polytetrafluorethylene sheets is recommended.

Test Procedure and Measurements

In designing the test procedure and making measurements, the following should be ensured:

- The tests must be performed under displacement control at a rate lower than 0.3 mm/min to ensure all the phases of the tests are clearly captured.
- LVDTs or potentiometers must be used to measure the relative slip between matrix and fabric. Other methods such as digital image correlation (DIC) can be used. It is important to evaluate the variability of the results and to take into account the influence of test setup and test rate, particularly the decreasing phase of the test.

Analysis of Results

When analyzing the results, the most significant parameters to define the mechanical behavior of FRCM are the analysis of the failure mode and the determination of the effective bond length. The efficiency of the reinforcement can be evaluated as the effectiveness ratio, which is defined as the stress at failure in the fabric versus its tensile strength (ratio of use of the mechanical properties of the fabric with respect to the bond properties).

Conclusions

The bond properties of different FRCM systems applied on masonry and concrete substrates were experimentally investigated using push-pull single-lap and double-lap shear test setups. The systems were composed of glass, carbon, and PBO fabrics embedded in their specific mortars. The influence of the bond length and mechanical properties of the component materials was described. The most common failure mode was slippage of the fabric within the matrix, and in some cases the tensile failure of the fabric. No debonding of the FRCM system from the substrate was observed.

Knowledge of the bond properties of a FRCM is needed to design the strengthening of a masonry or concrete structure. For this reason, standardization of the experimental procedure and a definition of the main design parameters are critical. The experimental results obtained were used to present a proposal for inclusion in guidelines and acceptance criteria. In particular, the geometry of the reinforcement (bond length and bond width), curing conditions, and test setup were described. To perform a complete characterization of FRCM systems, both tensile and bond tests are required. The first test provides an understanding of uniaxial tensile behavior, and the bond test provides an understanding of the shear behavior and adhesion properties between mortar and fabric. The values obtained from these experimental tests are not suitable for design of the strengthening of structural elements but are necessary in order to complete knowledge of the FRCM mechanical behavior.

Acknowledgments

The authors gratefully acknowledge the National Science Foundation (NSF) for the support provided to the Industry/University Center for Integration of Composites into Infrastructure (CICI) under Grant No. IIP-1439543 and its industrial members. Any opinions, findings, and conclusions or recommendations expressed in this material are those of the authors and do not necessarily reflect the views of the NSF. Part of the analyses were developed within the activities of Rete dei Laboratori Universitari di Ingegneria Sismica (ReLUIS) for the research program funded by the Dipartimento di Protezione Civile–Progetto Esecutivo 2014. Part of the experimental tests were performed at the Laboratorio Prove Materiali of the Politecnico di Milano, and their support is gratefully acknowledged.

References

Aiello, M. A., and S. M. Sciolti. 2006. "Bond analysis of masonry structures strengthened with CFRP sheets." *Constr. Build. Mater.* 20 (1–2): 90–100. https://doi.org/10.1016/j.conbuildmat.2005.06.040.

Arboleda, D., F. G. Carozzi, A. Nanni, and C. Poggi. 2015. "Testing procedures for the uniaxial tensile characterization of fabric-reinforced cementitious matrix composites." *J. Compos. Constr.* 20 (3): 04015063. https://doi.org/10.1061/(ASCE)CC.1943-5614.0000626.

Banholzer, B. 2004. "Bond behaviour of a multi-fiber yarn embedded in a cementitious matrix." Ph.D. thesis, Dept. of Civil Engineering, Aachen Univ.

Banholzer, B., W. Brameshuber, and W. Jung. 2006. "Analytical evaluation of pull-out tests—The inverse problem." *Cem. Concr. Compos.* 28 (6): 564–571. https://doi.org/10.1016/j.cemconcomp.2006.02.015.

Briccoli Bati, S. B., and M. Fagone. 2010. "An analysis of CFRP-brick bonded joints." In *Proc., XVIII GIMC Conf.* Siracusa, Italy: Gruppo Italiano di Meccanica Computazionale.

Caggegi, C., F. G. Carozzi, S. De Santis, F. Fabbrocino, and L. Zuccarino. 2017. "Experimental analysis on tensile and bond properties of PBO and aramid fabric reinforced cementitious matrix for strengthening masonry structures." *Composites Part B* 127 (Oct): 175–195. https://doi.org/10.1016/j.compositesb.2017.05.048.

Capozucca, R. 2010. "Experimental FRP/SRP–historic masonry delamination." *Compos. Struct.* 92 (4): 891–903. https://doi.org/10.1016/j.compstruct.2009.09.029.

Carbone, I. 2014. "Delaminazione di compositi a matrice cementizia su supporti murari." Ph.D. thesis, Engineering Dept., Università degli Studi Roma Tre.

Carloni, C., and F. Focacci. 2016. "FRP-masonry interfacial debonding: An energy balance approach to determine the influence of the mortar joints." *Eur. J. Mech.* 55 (Jan): 122–133. https://doi.org/10.1016/j.euromechsol.2015.08.003.

Carozzi, F. G., A. Bellini, T. D'Antino, G. de Felice, and C. Poggi. 2017. "Experimental investigation of tensile and bond properties of Carbon-FRCM composites for strengthening masonry elements." *Composites Part B* 128 (Nov): 100–119. https://doi.org/10.1016/j.compositesb.2017.06.018.

Carozzi, F. G., P. Colombi, G. Fava, and C. Poggi. 2016. "A cohesive interface crack model for the matrix–textile debonding in FRCM composites." *Compos. Struct.* 143 (May): 230–241. https://doi.org/10.1016/j.compstruct.2016.02.019.

Carozzi, F. G., P. Colombi, and C. Poggi. 2015. "Calibration of end-debonding strength model for FRP-reinforced masonry." *Compos. Struct.* 120 (Feb): 366–377. https://doi.org/10.1016/j.compstruct.2014.09.033.

Carozzi, F. G., G. Milani, and C. Poggi. 2014. "Mechanical properties and numerical modeling of fabric reinforced cementitious matrix (FRCM) systems for strengthening of masonry structures." *Compos. Struct.* 107 (Jan): 711–725. https://doi.org/10.1016/j.compstruct.2013.08.026.

Carozzi, F. G., and C. Poggi. 2015. "Mechanical properties and debonding strength of fabric reinforced cementitious matrix (FRCM) systems for masonry strengthening." *Composites Part B* 70 (Mar): 215–230. https://doi.org/10.1016/j.compositesb.2014.10.056.

Carrara, P., and F. Freddi. 2014. "Statistical assessment of a design formula for the debonding resistance of FRP reinforcements externally glued on masonry units." *Composites Part B* 66 (Nov): 65–82. https://doi.org/10.1016/j.compositesb.2014.04.032.

CEN (European Committee for Standardization). 2007. *Methods of test for mortar for masonry—Part 11: Determination of flexural and compressive strength of hardened mortar.* UNI EN 1015-11. Brussels, Belgium: CEN.

Ceroni, F., B. Ferracuti, M. Pecce, and M. Savoia. 2014. "Assessment of a bond strength model for FRP reinforcement externally bonded over masonry blocks." *Composites Part B* 61 (May): 147–161. https://doi.org/10.1016/j.compositesb.2014.01.028.

CNR (Consiglio Nazionale delle Ricerche). 2013. "Istruzioni per la Progettazione, l'Esecuzione e il Controllo di Interventi di Consolidamento Statico mediante l'utilizzo di Compositi Fibrorinforzati." In *Materiali, strutture di c.a. e di c.a.p., strutture murarie*. Roma: CNR.

Colombi, P., G. Fava, and C. Poggi. 2014. "End debonding of CFRP wraps and strips for the strengthening of concrete structures." *Compos. Struct.* 111 (May): 510–521. https://doi.org/10.1016/j.compstruct.2014.01.029.

D'Ambrisi, A., L. Feo, and F. Focacci. 2012. "Bond-slip relations for PBO-FRCM materials externally bonded to concrete." *Composites Part B* 43 (8): 2938–2949. https://doi.org/10.1016/j.compositesb.2012.06.002.

D'Ambrisi, A., L. Feo, and F. Focacci. 2013. "Experimental analysis on bond between PBO-FRCM strengthening materials and concrete." *Composites Part B* 44 (1): 524–532. https://doi.org/10.1016/j.compositesb.2012.03.011.

D'Antino, T. 2014. "Bond behavior in fiber reinforced polymer composites and fiber reinforced cementitious matrix composites." Ph.D. thesis, Dept. of Civil, Environmental and Architectural Engineering, Università di Padova.

D'Antino, T., C. Carloni, L. H. Sneed, and C. Pellegrino. 2014. "Matrix–fiber bond behavior in PBO FRCM composites: A fracture mechanics approach." *Eng. Fract. Mech.* 117 (Feb): 94–111. https://doi.org/10.1016/j.engfracmech.2014.01.011.

D'Antino, T., and C. Pellegrino. 2014. "Bond between FRP composites and concrete: Assessment of design procedures and analytical models." *Composites Part B* 60 (Apr): 440–456. https://doi.org/10.1016/j.compositesb.2013.12.075.

D'Antino, T., C. Pellegrino, C. Carloni, L. H. Sneed, and G. Giacomin. 2015. "Experimental analysis of the bond behavior of glass, carbon, and steel FRCM composites." *Key Eng. Mater.* 624 (Jan): 371–378. https://doi.org/10.4028/www.scientific.net/KEM.624.371.

de Felice, G., S. De Santis, L. Garmendia, B. Ghiassi, P. Larrinaga, P. B. Lourenço, and C. G. Papanicolaou. 2014. "Mortar-based systems for externally bonded strengthening of masonry." *Mater. Struct.* 47 (12): 2021–2037. https://doi.org/10.1617/s11527-014-0360-1.

De Santis, S., F. G. Carozzi, G. de Felice, and C. Poggi. 2017. "Test methods for textile reinforced mortar systems." *Composites Part B* 127 (Oct): 121–132. https://doi.org/10.1016/j.compositesb.2017.03.016.

Dvorkin, D., A. Poursaee, A. Peled, and W. J. Weiss. 2013. "Influence of bundle coating on the tensile behavior, bonding, cracking and fluid transport of fabric cement-based composites." *Cem. Concr. Compos.* 42 (Sep): 9–19. https://doi.org/10.1016/j.cemconcomp.2013.05.005.

Focacci, F., T. D'Antino, C. Carloni, L. H. Sneed, and C. Pellegrino. 2017. "An indirect method to calibrate the interfacial cohesive material law for FRCM-concrete joints." *Mater. Des.* 128 (Aug): 206–217. https://doi.org/10.1016/j.matdes.2017.04.038.

ISO. 2005. *Carbon fibre—Determination of tensile properties of resin-impregnated yarn*. EN ISO 10618. London: ISO.

ISO. 2011. *Hexalobular socket cheese head screws*. UNI EN ISO 14580. Geneva: ISO.

Kwiecień, A. 2012. "Stiff and flexible adhesives bonding CFRP to masonry substrates—Investigated in pull-off test and single-lap test." *Arch. Civ. Mech. Eng.* 12 (2): 228–239. https://doi.org/10.1016/j.acme.2012.03.015.

Leone, M., et al. 2017. "Glass fabric reinforced cementitious matrix: Tensile properties and bond performance on masonry substrate." *Composites Part B* 127 (Oct): 196–214. https://doi.org/10.1016/j.compositesb.2017.06.028.

Lu, X. Z., J. G. Teng, L. P. Ye, and J. J. Jiang. 2005. "Bond–slip models for FRP sheets/plates bonded to concrete." *Eng. Struct.* 27 (6): 920–937. https://doi.org/10.1016/j.engstruct.2005.01.014.

Malena, M., and G. de Felice. 2014. "Debonding of composites on a curved masonry substrate: Experimental results and analytical formulation." *Compos. Struct.* 112 (Jun): 194–206. https://doi.org/10.1016/j.compstruct.2014.02.004.

Mostofinejad, D., and A. Tabatabaei Kashani. 2013. "Experimental study on effect of EBR and EBROG methods on debonding of FRP sheets used for shear strengthening of RC beams." *Composites Part B* 45 (1): 1704–1713. https://doi.org/10.1016/j.compositesb.2012.09.081.

Mukhtar, F. M., and R. M. Faysal. 2018. "A review of test methods for studying the FRP-concrete interfacial bond behavior." *Constr. Build. Mater.* 169 (Apr): 877–887. https://doi.org/10.1016/j.conbuildmat.2018.02.163.

Peled, A., E. Zaguri, and G. Marom. 2008. "Bonding characteristics of multifilament polymer yarns and cement matrices." *Composites Part A* 39 (6): 930–939. https://doi.org/10.1016/j.compositesa.2008.03.012.

Valluzzi, M. R., D. V. Oliveira, A. Caratelli, G. Castori, M. Corradi, G. de Felice, and G. Zuccarino. 2012. "Round robin test for composite-to-brick shear bond characterization." *Mater. Struct.* 45 (12): 1761–1791. https://doi.org/10.1617/s11527-012-9883-5.